Received: 11 April 2024 | Revised: 19 July 2024 | Accepted: 1 August 2024

DOI: 10.1111/cas.16315

Cancer Science WILEY

ORIGINAL ARTICLE

Fusobacterium nucleatum, immune responses, and metastatic organ diversity in colorectal cancer liver metastasis

Yasuyuki Shigematsu[1,2] | Rumiko Saito[3,4,5] | Gulanbar Amori[1,2,6] | Hiroaki Kanda[7] | Yu Takahashi[8] | Kengo Takeuchi[1,2,9] | Shunji Takahashi[3,4] | Kentaro Inamura[1,2,6]

[1]Department of Pathology, Cancer Institute Hospital, Japanese Foundation for Cancer Research, Tokyo, Japan

[2]Division of Pathology, Cancer Institute, Japanese Foundation for Cancer Research, Tokyo, Japan

[3]Department of Medical Oncology, Cancer Institute Hospital, Japanese Foundation for Cancer Research, Tokyo, Japan

[4]Department of Clinical Chemotherapy, Cancer Chemotherapy Center, Japanese Foundation for Cancer Research, Tokyo, Japan

[5]Graduate School of Engineering, Chiba Institute of Technology, Chiba, Japan

[6]Division of Tumor Pathology, Jichi Medical University, Tochigi, Japan

[7]Department of Pathology, Saitama Cancer Center, Saitama, Japan

[8]Division of Hepatobiliary and Pancreatic Surgery, Cancer Institute Hospital, Japanese Foundation for Cancer Research, Tokyo, Japan

[9]Pathology Project for Molecular Targets, Cancer Institute, Japanese Foundation for Cancer Research, Tokyo, Japan

Correspondence
Kentaro Inamura, Division of Pathology, Cancer Institute, Japanese Foundation for Cancer Research, 3-8-31, Ariake, Koto-ku, Tokyo 135-8550, Japan.
Email: inamura-tky@umin.ac.jp

Funding information
Japan Society for the Promotion of Science, Grant/Award Number: JP22H02930, JP23K14491 and JP23K18246; Yakult Bio-Science Foundation

Abstract

The presence of *Fusobacterium nucleatum* is associated with an immunosuppressive tumor immune microenvironment (TIM) in primary colorectal cancer (CRC), contributing to tumor progression. Its persistence in CRC liver metastasis tissues raises questions about its role in modulating local and systemic immune responses and influencing recurrence patterns. This retrospective cohort study of 218 patients with CRC liver metastasis investigated the association of *F. nucleatum* in CRC liver metastasis tissues with systemic inflammation, TIM alterations, and the number of metastatic organs involved in recurrence. Two-step polymerase chain reaction (PCR), including digital PCR, detected *F. nucleatum* in 42% (92/218) of fresh-frozen specimens of CRC liver metastases. Compared with the *F. nucleatum*-none group, the *F. nucleatum*-high group showed higher C-reactive protein levels (0.82 vs. 0.22 mg/dL; $P_{trend}=0.02$), lower numbers of $CD8^+$ cells (33.2 vs. 65.3 cells/mm^2; $P_{trend}=0.04$) and $FOXP3^+$ cells (11.3 vs. 21.7 cells/mm^2; $P_{trend}=0.01$) in the TIM, and a greater number of metastatic organs involved in recurrence (1.6 vs. 1.1; $p<0.001$). The presence of *F. nucleatum* in CRC liver metastasis tissues was associated with increased systemic inflammation, TIM alterations, and a greater number of metastatic organs involved in recurrence. These findings suggest a potential contribution of *F. nucleatum* to the metastatic

Abbreviations: ANOVA, analysis of variance; CI, confidence interval; CRC, colorectal cancer; CRP, C-reactive protein; DFS, disease-free survival; dMMR, deficient mismatch repair; FFPE, formalin-fixed paraffin-embedded; HSD, honestly significant difference; OS, overall survival; PCR, polymerase chain reaction; TIM, tumor immune microenvironment; TMA, tissue microarray.

Yasuyuki Shigematsu and Rumiko Saito contributed equally to this work and share first authorship.

propensity of CRC cells and could inform future research to enhance understanding of the interaction between tumor, host, and microbes in the metastatic process.

KEYWORDS
colorectal cancer, *Fusobacterium nucleatum*, liver metastasis, systemic inflammation, tumor-immune microenvironment

1 | INTRODUCTION

Colorectal cancer (CRC) is the third most common cancer and the second leading cause of cancer-related death worldwide.[1,2] Approximately 35%–55% of patients diagnosed with CRC eventually develop liver metastasis,[3] which is responsible for over 60% of CRC-related deaths.[4,5] Although surgical resection of liver metastases is recommended in cases of potentially curable CRC, the recurrence rates range from 50% to 70%.[6–8] This underscores the need to elucidate the factors involved in the metastatic progression of CRC, particularly in the liver.

The hepatic tumor immune microenvironment (TIM) provides premetastatic niches, facilitating CRC cell implantation and proliferation.[9] Concurrently, systemic inflammation exacerbates CRC progression and metastasis by promoting angiogenesis and increasing vascular permeability.[10] Elevated levels of serum C-reactive protein (CRP) have been shown to be an adverse prognostic indicator in CRC liver metastasis.[11] Furthermore, the number of organs with metastases influences the prognosis of patients with metastatic CRC.[12] Despite these insights into the complex interplay between hepatic TIM, systemic inflammation, and CRC liver metastasis, the mechanisms driving these associations remain elusive and warrant further investigation.

Advancements in metagenomic analysis have demonstrated the role of intratumoral bacteria in modulating immune responses across various tumor types.[13–15] *Fusobacterium nucleatum*, an oral commensal bacterium, is enriched in primary CRC tissues compared with adjacent noncancerous tissues[16,17] and is recognized as a key member of CRC-associated bacteria.[18,19] In primary CRC tissues, *F. nucleatum* suppresses T-cell activity in the TIM and is associated with tumor cell features, such as high-level microsatellite instability.[13,20–22] A recent study that used a mouse model of CRC liver metastasis found that oral administration of *F. nucleatum* modulates the hepatic immune environment and upregulates proinflammatory cytokines in the plasma.[23] Notably, *F. nucleatum* in primary CRC tissues accompanies metastasizing CRC cells to the liver, maintaining its presence in CRC liver metastasis tissues.[24,25] This raises questions about the role of *F. nucleatum* in shaping systemic and local immune responses and its effect on the recurrence patterns in CRC liver metastasis.

This study evaluated the association of *F. nucleatum* in CRC liver metastasis tissues with systemic and local immune responses, and the diversity of metastatic organs involved in recurrence. Using fresh-frozen samples for quantifying *F. nucleatum* DNA, formalin-fixed paraffin-embedded (FFPE) specimens for evaluating the TIM, and clinical data on serum CRP levels and metastatic organs involved in recurrence after R0 metastasectomy, the potential role of *F. nucleatum* in the complex dynamics of CRC liver metastasis was explored.

2 | MATERIALS AND METHODS

2.1 | Patients and specimens

Surgical specimens were obtained from consecutive patients with CRC liver metastasis who underwent curative-intent R0 metastasectomy at the Cancer Institute Hospital in Tokyo, Japan between January 2005 and December 2015. All the samples were collected from surgically resected metastatic liver lesions. The resected tissues were divided and preserved as frozen and FFPE specimens. All fresh samples were grossly dissected and snap frozen in liquid nitrogen within 20 min of removal. The inclusion criteria in this study were the availability of sufficient fresh-frozen and FFPE specimens, along with complete pathological records. A total of 218 patients with CRC liver metastasis were included in this study. Clinicopathological data, including age, sex, preoperative blood data, tumor location, number of liver metastases, history of chemotherapy, and number of metastatic organs involved in recurrence, were extracted from the electronic medical records. The medical records of all patients with CRC liver metastasis included in this study were reviewed by study physicians. The study protocol was approved by the Ethics Committee of the Japanese Foundation for Cancer Research (approval number: 2016-1087). The requirement for informed consent was waived due to the retrospective nature of the study.

2.2 | Pathological evaluation

Tissue sections (4-μm thickness) from FFPE samples were stained using hematoxylin and eosin. CRC liver metastasis was confirmed by two pathologists (YS and KI) according to the criteria of the fifth edition of the World Health Organization guidelines.[26]

2.2.1 | Tissue microarray (TMA)

A TMA was constructed using the FFPE tumor specimens[27] to evaluate the tumor and tumor-infiltrating cells immunohistochemically.

Briefly, specific regions of the donor paraffin blocks were extracted using a 2-mm coring needle, and these regions were then transferred onto an array in the recipient block with the assistance of a KIN-1 manual tissue arrayer (Azumaya). For each tumor, three tissue cores representing the predominant histology of the tumor were selected. The 4-μm-thick TMA sections were used for the immunohistochemical evaluation, as described below.

2.2.2 | Immunohistochemistry

Immunohistochemistry of the tumor cells was performed using anti-MLH1 (1:100; clone ES05; Leica Biosystems), anti-MSH2 (1:500; clone G219-1129; BD Bioscience), anti-MSH6 (1:500; clone EPR3945; Abcam), and anti-PMS2 (1:100; clone A16-4; BD Bioscience) mouse monoclonal antibodies. Immune cell infiltrations in TIM were evaluated using anti-CD8 (1:3; clone C8/144B; Nichirei), anti-CD4 (1:2; clone 4B12; Nichirei), anti-CD20 (1:800; clone L26; Leica Biosystems), anti-FOXP3 (1:100; clone 236A/E7; Abcam), anti-CD163 (1:1200; clone 10D6; Leica Biosystems), and anti-CD68 (1:1000, clone KP-1; Dako) mouse monoclonal antibodies. Noncancerous liver tissues from the same TMA sections, including hepatocytes, bile ducts, lymphocytes, and nerves, were used as positive and negative controls. Immunostaining was performed using a Bond-III automated staining system (Leica Microsystems), and antigen was detected using the Bond Polymer Refine Detection Kit (Leica Microsystems).

2.2.3 | Antigen retrieval for immunohistochemistry

CD68 antigens were activated by incubation with a 200-fold dilution of protease K for 5 min. All other antigens were activated by heating at 100°C for 20 min in an ethylenediaminetetraacetic acid (EDTA)-surfactant buffer (pH 9.0).

2.3 | Evaluation of the immunohistochemistry variables in the TMA

The expression of MLH1, PMS2, MSH2, and MSH6 were used as markers of mismatch repair protein expression. Loss of mismatch repair protein was defined as the absence of nuclear expression in tumor cells with positive nuclear expression in lymphocytes. We evaluated three tissue cores per tumor for each protein expression analysis and the tumor was considered to have lost its protein expression if all three tissue cores lacked protein expression. The loss of any of the four mismatch repair proteins in tumor cells was defined as deficient mismatch repair (dMMR). Two pathologists (YS and KI) scored all cases blindly and independently, and cases that were difficult to interpret immunohistochemically were reviewed by a third pathologist (HK).

To evaluate the number of tumor-infiltrating immune cells, immunostained sections were digitized and mechanically quantified as described previously.[28] Briefly, immunostained sections at ×40 magnification were scanned using a NanoZoomer Digital Pathology System (Hamamatsu Photonics KK) with a resolution of 0.55 pixel/μm. The images were then semiautomatically digitized using the proprietary NanoZoomer Digital Pathology Image file format. Fiji, an open-source platform for biological image analysis,[29] was used to quantify the number of tumor-infiltrating immune cells. A microscopic field of each tissue core was selected from the scanned TMA images, and the images were analyzed using Fiji to count the number of tumor-infiltrating immune cells. Three tissue cores were evaluated for each tumor, and the mean number of tumor-infiltrating immune cells was calculated to determine their number in the tumor.

2.4 | DNA extraction and quantitative PCR for *F. nucleatum* quantification

DNA was extracted from fresh-frozen CRC liver metastasis tissue specimens using the NucleoSpin Tissue Kit (Takara Bio Inc.) and quantified using a Nanodrop ND-1000 spectrophotometer (Thermo Fisher Scientific Inc.). The initial polymerase chain reaction (PCR) was conducted using 25 μL of sample solution comprising 100 ng of extracted DNA and specific primers designed to detect *F. nucleatum*-specific sequences (Table S1). The initial PCR assay for *F. nucleatum* involved an initial denaturation step at 95°C for 10 min, followed by 40 cycles, with denaturation at 95°C for 15 s, followed by annealing and extension at 60°C for 1 min. For quantification, the initial PCR product of *F. nucleatum* was diluted 10^6-fold and subjected to EvaGreen-based Droplet Digital PCR using 1 μL volume of the diluted sample. To determine the relative amount of *F. nucleatum* DNA in a sample based on the quantity of input gDNA, the EvaGreen-based Droplet Digital PCR was used on samples comprising 10 ng of gDNA with specific primers for the reference human gene *SLCO2A1* (Table S1). The EvaGreen-based Droplet Digital PCR conditions for *F. nucleatum* and *SLCO2A1* included an initial denaturation step at 95°C for 10 min, followed by 40 and 35 cycles, respectively, with denaturation at 95°C for 15 s, followed by annealing and extension at 60°C for 1 min. The Droplet Digital PCR method was carried out with the QX200 Droplet Digital PCR System (Bio-Rad Laboratories, Inc.) using EvaGreen assays. To ensure the accuracy and reliability of *F. nucleatum* DNA quantification, we adhered to the recommended contamination control guidelines for low-biomass microbiome research.[30]

2.5 | Statistical analysis

All statistical analyses were performed using R version 4.2.3 (R Foundation for Statistical Computing). Cases with detectable *F.*

nucleatum DNA were divided into low and high groups based on the median cut point of the relative amount of *F. nucleatum* DNA, whereas cases that did not have any detectable *F. nucleatum* DNA were assigned to the "none" group. Continuous variables were reported as means and standard deviations. Categorical variables were reported as numbers and percentages. Welch's *t*-test was used to compare the mean values of two groups, and one-way analysis of variance (ANOVA) was used to compare the mean values of three groups. Post hoc comparisons were performed using Tukey's honest significant difference (HSD) test to determine the specific pairs of groups with significant differences. Categorical variables were compared using Fisher's exact test. An ordinal logistic regression model was used to assess the association between the amount of *F. nucleatum* DNA in liver metastasis tissues (an ordinal predictor variable) and the density of tumor-infiltrating immune cells. Survival analysis was conducted using the Kaplan–Meier method to plot disease-free survival (DFS) and overall survival (OS) curves stratified by the amount of *F. nucleatum* present in CRC liver metastasis tissues. The log-rank test was used to assess the statistical significance of differences in survival between groups. Two-tailed *p*-values <0.05 were considered statistically significant.

3 | RESULTS

3.1 | *Fusobacterium nucleatum* in CRC liver metastasis tissues

We quantified *F. nucleatum* DNA in tumor tissues obtained from 218 patients with CRC liver metastasis. *F. nucleatum* DNA was detected in 92 (42%) of these cases, leading to the classification of 46 cases into *F. nucleatum*-low and -high groups based on their relative DNA amounts. The remaining 126 cases, in which *F. nucleatum* DNA was undetectable, were categorized as *F. nucleatum*-none. *F. nucleatum* was detected in five of the seven tumors with dMMR ($p = 0.01$; Table 1), confirming the association between the amount of *F. nucleatum* and dMMR in CRC liver metastases. In a secondary analysis, we investigated the presence of *F. nucleatum* in the primary tumors of 15 patients with CRC and synchronous liver metastases

TABLE 1 Clinicopathological features according to the amount of *Fusobacterium nucleatum* present in CRC liver metastasis tissues.

Variable	Total ($n = 218$)	Amount of *F. nucleatum* DNA in CRC liver metastatic tissues			*p*-Value
		None ($n = 126$)	Low ($n = 46$)	High ($n = 46$)	
Age (years)[b]	62.7 (±11.1)	63.2 (±10.9)	61.5 (±11.0)	62.4 (±11.9)	0.65
Sex[a]					
Female	81 (37.2)	47 (37.3)	17 (37.0)	17 (37.0)	>0.99
Male	137 (62.8)	79 (62.7)	29 (63.0)	29 (63.0)	
Number of metastases[b]	4.7 (±7.1)	4.3 (±6.5)	6.1 (±8.2)	4.6 (±7.4)	0.34
Primary tumor location[a]					
Right side	46 (21.1)	27 (21.4)	10 (21.7)	9 (19.6)	>0.99
Left side	172 (78.9)	99 (78.6)	36 (78.3)	37 (80.4)	
History of chemotherapy[a]					
None	124 (56.9)	77 (61.1)	20 (43.5)	27 (58.7)	0.12
Done	94 (43.1)	49 (38.9)	26 (56.5)	19 (41.3)	
Timing of metastasis[a]					
Synchronous	116 (53.2)	62 (49.2)	27 (58.7)	27 (58.7)	0.40
Metachronous	102 (46.8)	64 (50.8)	19 (41.3)	19 (41.3)	
Tumor differentiation[a]					
Well to moderate	208 (95.4)	120 (95.2)	44 (95.7)	44 (95.6)	0.96
Poor	10 (4.6)	6 (4.8)	2 (4.3)	2 (4.3)	
Mismatch repair protein[a]					
Intact	211 (96.8)	124 (98.4)	46 (100)	41 (89.1)	0.01
Deficient	7 (3.2)	2 (1.6)	0 (0)	5 (10.9)	

Abbreviation: CRC, colorectal cancer.

[a]Data presented as mean (± standard deviation).

[b]Data presented as number (%).

in which *F. nucleatum* had been detected (eight samples from the *F. nucleatum*-low group, and seven samples from the *F. nucleatum*-high group). Using FFPE samples and the two-step PCR-based method, we detected *F. nucleatum* in all 15 samples. These results support the hypothesis that *F. nucleatum* may disseminate from the primary tumor to the liver with metastatic CRC cells.

3.2 | *Fusobacterium nucleatum* in CRC liver metastasis tissues and systemic immune responses

C-reactive protein is an indicator of systemic inflammation. In this study, the CRP levels were positively associated with the increase in the amount of *F. nucleatum* DNA in CRC liver metastases ($P_{trend}=0.02$) (Figure 1). The *F. nucleatum*-high group showed higher CRP levels than the *F. nucleatum*-none group (mean: 0.82 vs. 0.22 mg/dL; $p=0.02$). These findings indicate an association between the presence of *F. nucleatum* at metastatic sites and increased systemic inflammation. However, no statistically significant association was observed between the amount of *F. nucleatum* present in CRC liver metastasis tissues and the blood lymphocyte count (mean lymphocyte count: 1581.1 cells/μL in the *F. nucleatum*-none, 1525.4 cells/μL in the *F. nucleatum*-low, and 1796.2 cells/μL in the *F. nucleatum*-high groups; $P_{trend}=0.16$).

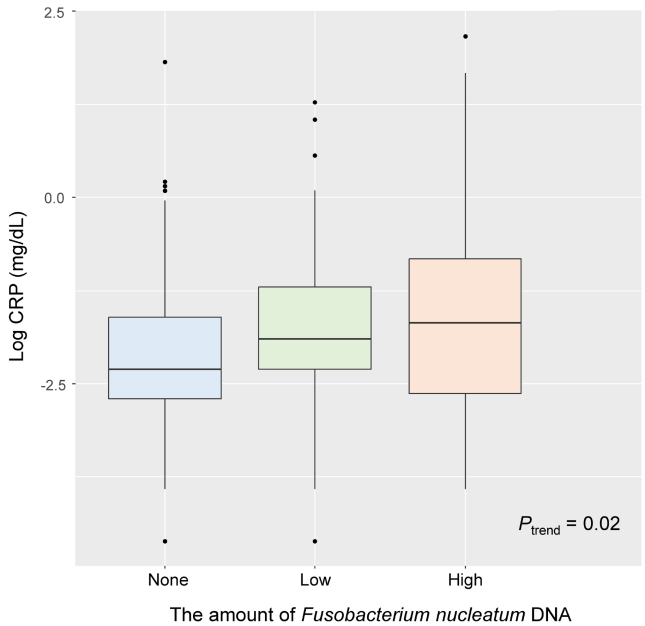

FIGURE 1 Box plots showing the trend in log-transformed C-reactive protein (CRP) levels grouped by the amount of *Fusobacterium nucleatum* DNA: "None" in pale blue, "Low" in pale green, and "High" in pale orange. The box plots indicate an increasing trend in preoperative serum CRP levels across the different *F. nucleatum* DNA groups ($P_{trend}=0.02$), suggesting a positive association between the amount of *F. nucleatum* DNA present in colorectal cancer liver metastasis tissues and systemic inflammation.

3.3 | *Fusobacterium nucleatum* and the TIM in CRC liver metastasis tissues

Tumor-infiltrating immune cells were relatively homogeneous and were generally either diffuse or aggregated in each TMA tissue core. Tumor-infiltrating immune cells were characterized immunohistochemically as $CD8^+$, $CD4^+$, $CD20^+$, $FOXP3^+$, $CD163^+$, and $CD68^+$ cells and the density of each cell type was quantified in tumor tissues. The number of $CD8^+$ cells and $FOXP3^+$ cells decreased with an increase in *F. nucleatum* DNA levels in CRC liver metastasis tissues ($P_{trend}=0.04$ for $CD8^+$ cells and $P_{trend}=0.01$ for $FOXP3^+$ cells; Table 2). Compared with the *F. nucleatum*-none group, the *F. nucleatum*-high group had fewer $CD8^+$ cells ($p=0.001$) and $FOXP3^+$ cells ($p<0.001$). In a secondary analysis of 21 randomly selected cases (seven cases each from the *F. nucleatum*-none, -low, and -high groups), we observed similar trends in the association between the amount of *F. nucleatum* present in FFPE specimens and the abundance of tumor-infiltrating immune cells (Table S2).

3.4 | *Fusobacterium nucleatum* in CRC liver metastasis tissues and the number of metastatic organs involved

To assess the propensity of extracolonic metastasis to recur after R0 resection with hepatic metastasectomy, we evaluated the number of organs involved in 136 cases with recurrence. Among these cases, there were 78, 32, and 26 cases in the *F. nucleatum*-none, -low, and -high groups, respectively. Across the *F. nucleatum*-none, -low, and -high groups, the number of metastatic organs involved in recurrence increased according to the amount of *F. nucleatum* present ($p<0.001$, ANOVA; Figure 2). Post hoc pairwise comparisons using Tukey's HSD test indicated significant differences between the *F. nucleatum*-none and -high groups (mean difference = 0.54, $p=0.001$), and between the *F. nucleatum*-low and -high groups (mean difference = 0.40, $p=0.02$). Notably, one of 26 patients (4%) in the *F. nucleatum*-high group had recurrent lesions in the liver, lung, lymph nodes, peritoneum, and spleen on confirmation of recurrence.

3.5 | *Fusobacterium nucleatum* in CRC liver metastasis tissues and survival

In an exploratory analysis, we did not observe a significant association between the amount of *F. nucleatum* present in CRC liver metastasis tissues and either DFS or OS (DFS: log-rank $p=0.35$, OS: log-rank $p=0.72$; Figure S1).

4 | DISCUSSION

Using a highly sensitive method to detect *F. nucleatum* DNA, we detected *F. nucleatum* in CRC liver metastasis tissues in over one-third

TABLE 2 Density of tumor-infiltrating immune cells according to the amount of *Fusobacterium nucleatum* present in CRC liver metastasis tissues.

Cell type	Amount of *F. nucleatum* DNA present in CRC liver metastasis			*p*-Value for trend
	None ($n=126$)	Low ($n=46$)	High ($n=46$)	
$CD8^+$ cells	65.3 (±89.1)	61.4 (±72.7)	33.2 (±35.9)	0.04
$CD4^+$ cells	47.2 (±97.8)	39.6 (±59.2)	29.2 (±38.7)	0.87
$CD20^+$ cells	14.1 (±36.4)	5.5 (±8.2)	6.4 (±15.7)	0.26
$FOXP3^+$ cells	21.7 (±28.8)	16.8 (±13.9)	11.3 (±9.7)	0.01
$CD163^+$ cells	150.0 (±186.0)	146.3 (±164.4)	118.0 (±104.8)	0.59
$CD68^+$ cells	221.6 (±242.1)	207.4 (±263.3)	127.6 (±162.9)	0.06

Note: Data presented as mean (±standard deviation) cell count per mm^2.
Abbreviation: CRC, colorectal cancer.

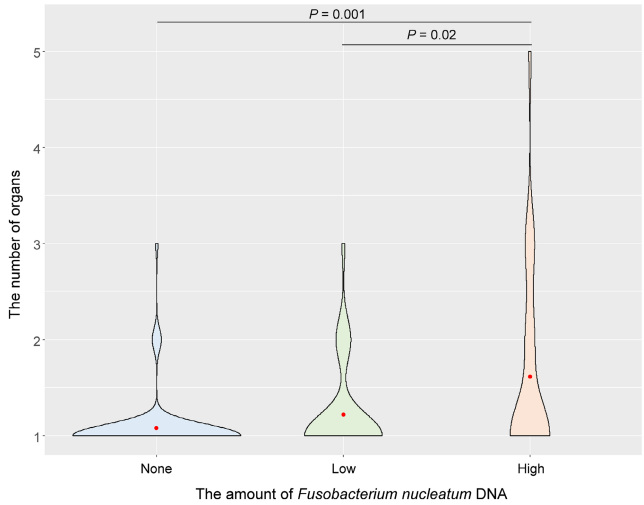

FIGURE 2 Violin plots illustrating the distribution of the number of organs involved in recurrence grouped by the amount of *Fusobacterium nucleatum* DNA: "None" in pale blue, "Low" in pale green, and "High" in pale orange. The red dots indicate the average organ count for each group. The "High" group shows a higher number of organs involved in recurrence, compared with the "None" ($p=0.001$) and "Low" ($p=0.02$) groups. *p*-Values were calculated using Tukey's honestly significant difference test.

of cases. We not only confirmed the presence of *F. nucleatum* in metastatic sites but also revealed its association with the systemic and local immune responses. The amount of *F. nucleatum* was associated with increased systemic inflammation, as indicated by elevated CRP levels, and TIM alterations, as indicated by reduced numbers of $CD8^+$ cells and $FOXP3^+$ cells. These changes might contribute to the observed diversity in the metastatic organs involved in recurrence, indicating that *F. nucleatum* might contribute to the metastatic propensity of CRC cells. Our findings provide a new perspective on the interactions between *F. nucleatum* and the host immunity in the complex dynamics of CRC metastasis.

Due to the challenges in detecting *F. nucleatum* in CRC liver metastasis tissues, particularly its low abundance and the limitations of the conventional detection techniques, its relationship to clinicopathological features remains largely unexplored. A previous study used FFPE specimens and single conventional real-time PCR and detected *F. nucleatum* in only 4.4% (8/181 cases) of CRC liver metastasis.[25] However, this study adopted a sensitive approach using fresh-frozen specimens and a digital PCR assay to extract the initial PCR products, thereby substantially increasing the detection rate to 42% (92/218 cases). This increased sensitivity enabled a more precise evaluation of the association between the presence of *F. nucleatum* in CRC liver metastasis tissues and various clinicopathological features, providing new insights into its potential influence on the metastatic progression of CRC.

Currently, the influence of *F. nucleatum* in CRC liver metastasis tissues on the TIM is poorly understood. In the primary CRC tissues of the $Apc^{Min/+}$ mouse model, *F. nucleatum* hinders T-cell-mediated antitumor responses by promoting the recruitment of specific myeloid cell subsets.[31] Furthermore, a population study involving nearly 600 patients with CRC found an inverse association between *F. nucleatum* abundance and the density of $CD3^+$ T cells in primary CRC tissues.[20] This study extends this narrative to CRC liver metastasis and demonstrates that the amount of *F. nucleatum* is associated with a reduced density of $CD8^+$ cells and $FOXP3^+$ cells. Given that $CD8^+$ cells recognize and eliminate CRC cells, the inverse association between the amount of *F. nucleatum* and the density of $CD8^+$ cells indicates that *F. nucleatum* might contribute to the suppression of cytotoxic T-cell activity in CRC liver metastases. Furthermore, considering that $FOXP3^+$ cells play a tumor-suppressive role in CRC tissues,[32] the observed reduction of $FOXP3^+$ cell density in *F. nucleatum*-positive metastasis tissues indicates a potential shift in the TIM toward a more tumor-promoting state, facilitating the establishment of premetastatic niches.[9] These observations underscore the potential of *F. nucleatum* to reshape the local immune responses, thereby facilitating CRC cell implantation and proliferation. Furthermore, *F. nucleatum* in CRC liver metastases was associated with increased systemic inflammation and diversity in metastatic organs involved in recurrence. These findings suggest that *F. nucleatum* might contribute to metastatic progression by modulating local and systemic immune responses. By altering the TIM and increasing systemic inflammation, *F. nucleatum* might facilitate the establishment of premetastatic niches in various organs beyond the liver. Further studies are warranted to investigate whether and how *F. nucleatum*

modulates immune responses and influences metastatic organ tropism. Insights from such studies could help develop potential strategies that target *F. nucleatum* and the related immune pathways and advance the management of metastatic CRC.

This study has several limitations. First, *F. nucleatum* was evaluated using fresh-frozen specimens obtained from one liver metastasis per patient. Although the results might not fully capture the variability across all metastatic lesions, efforts were made to minimize the sampling bias by selecting specimens from the largest metastatic lesion. Second, the use of TMA for immunohistochemical evaluation introduces limitations because of intratissue heterogeneity, which might not be representative of the overall tumor tissues. We investigated three tissue cores per tumor to encompass a broad range of the TIM. Third, the total number of patients was not large enough, and the statistical power was therefore limited. Fourth, we were unable to localize *F. nucleatum* within liver metastasis tissues due to challenges in detecting the bacterium using fluorescence in situ hybridization and similar methods. We were thus unable to validate our findings using non-PCR-based methods or to perform an analysis of the spatial relationship between *F. nucleatum* and tumor-infiltrating immune cells. Future research using advanced detection techniques could provide further insights into the spatial distribution of *F. nucleatum* and its interaction with immune cells within the TIM. Finally, the patient cohort was derived from a single cancer hospital in Japan, which might limit the generalizability of the results to other populations. Therefore, further investigation with larger and more diverse cohorts is required to confirm our findings.

In conclusion, this study demonstrated the interactions between *F. nucleatum* in CRC liver metastasis tissues, systemic inflammation, and TIM alterations. This interplay might contribute to the increased diversity of metastatic organs involved in recurrence. Further research is warranted to determine the clinical implications of these findings and to develop effective treatment strategies for metastatic CRC.[33–35]

AUTHOR CONTRIBUTIONS

Yasuyuki Shigematsu: Conceptualization; data curation; formal analysis; funding acquisition; investigation; methodology; writing – original draft; writing – review and editing. **Rumiko Saito:** Data curation; formal analysis; investigation; methodology; writing – review and editing. **Gulanbar Amori:** Methodology; writing – review and editing. **Hiroaki Kanda:** Methodology; writing – review and editing. **Yu Takahashi:** Methodology; resources; writing – review and editing. **Kengo Takeuchi:** Supervision; writing – review and editing. **Shunji Takahashi:** Supervision; writing – review and editing. **Kentaro Inamura:** Conceptualization; funding acquisition; investigation; methodology; project administration; supervision; writing – original draft; writing – review and editing.

ACKNOWLEDGMENTS

We thank Mr. Motoyoshi Iwakoshi and Dr. Shuhei Ishii for their kind assistance with sample preparation.

FUNDING INFORMATION

This work was supported by grants from JSPS KAKENHI (grant numbers JP22H02930 and JP23K18246 to KI and JP23K14491 to YS) and the Yakult Bio-Science Foundation (to KI).

CONFLICT OF INTEREST STATEMENT

Kengo Takeuchi is an editorial board member of *Cancer Science*. The other authors declare no competing interest.

DATA AVAILABILITY STATEMENT

The datasets used and/or analyzed during the current study are available from the corresponding author upon reasonable request.

ETHICS STATEMENTS

The study was approved by the Ethics Committee of the Japanese Foundation for Cancer Research (reference number: 2016-1087).

INFORMED CONSENT

The requirement for informed consent was waived because of the retrospective design of this study.

ORCID

Yasuyuki Shigematsu https://orcid.org/0000-0001-5142-2906
Kengo Takeuchi https://orcid.org/0000-0002-1599-5800
Kentaro Inamura https://orcid.org/0000-0001-6444-3861

REFERENCES

1. Sung H, Ferlay J, Siegel RL, et al. Global cancer statistics 2020: GLOBOCAN estimates of incidence and mortality worldwide for 36 cancers in 185 countries. *CA Cancer J Clin*. 2021;71(3):209-249. doi:10.3322/caac.21660
2. Morgan E, Arnold M, Gini A, et al. Global burden of colorectal cancer in 2020 and 2040: incidence and mortality estimates from GLOBOCAN. *Gut*. 2023;72(2):338-344. doi:10.1136/gutjnl-2022-327736
3. Pawlik TM, Choti MA. Surgical therapy for colorectal metastases to the liver. *J Gastrointest Surg*. 2007;11(8):1057-1077. doi:10.1007/s11605-006-0061-3
4. Welch JP, Donaldson GA. The clinical correlation of an autopsy study of recurrent colorectal cancer. *Ann Surg*. 1979;189(4):496-502. doi:10.1097/00000658-197904000-00027
5. Geoghegan JG, Scheele J. Treatment of colorectal liver metastases. *Br J Surg*. 1999;86(2):158-169. doi:10.1046/j.1365-2168.1999.01013.x
6. Fernandez FG, Drebin JA, Linehan DC, Dehdashti F, Siegel BA, Strasberg SM. Five-year survival after resection of hepatic metastases from colorectal cancer in patients screened by positron emission tomography with F-18 fluorodeoxyglucose (FDG-PET). *Ann Surg*. 2004;240(3):438-450. doi:10.1097/01.sla.0000138076.72547.b1
7. Nordlinger B, Guiguet M, Vaillant JC, et al. Surgical resection of colorectal carcinoma metastases to the liver. A prognostic scoring system to improve case selection, based on 1568 patients. Association Francaise de Chirurgie. *Cancer*. 1996;77(7):1254-1262. doi:10.1002/(sici)1097-0142(19960401)77
8. Yoon SS, Tanabe KK. Multidisciplinary management of metastatic colorectal cancer. *Surg Oncol*. 1998;7(3–4):197-207. doi:10.1016/s0960-7404(99)00022-5
9. Wang Y, Zhong X, He X, et al. Liver metastasis from colorectal cancer: pathogenetic development, immune landscape of the tumour

microenvironment and therapeutic approaches. *J Exp Clin Cancer Res*. 2023;42(1):177. doi:10.1186/s13046-023-02729-7
10. Tuomisto AE, Makinen MJ, Vayrynen JP. Systemic inflammation in colorectal cancer: underlying factors, effects, and prognostic significance. *World J Gastroenterol*. 2019;25(31):4383-4404. doi:10.3748/wjg.v25.i31.4383
11. Hamilton TD, Leugner D, Kopciuk K, Dixon E, Sutherland FR, Bathe OF. Identification of prognostic inflammatory factors in colorectal liver metastases. *BMC Cancer*. 2014;14:542. doi:10.1186/1471-2407-14-542
12. Rumpold H, Niedersuss-Beke D, Heiler C, et al. Prediction of mortality in metastatic colorectal cancer in a real-life population: a multicenter explorative analysis. *BMC Cancer*. 2020;20(1):1149. doi:10.1186/s12885-020-07656-w
13. Inamura K, Hamada T, Bullman S, Ugai T, Yachida S, Ogino S. Cancer as microenvironmental, systemic and environmental diseases: opportunity for transdisciplinary microbiomics science. *Gut*. 2022;71:2107-2122. doi:10.1136/gutjnl-2022-327209
14. El Tekle G, Garrett WS. Bacteria in cancer initiation, promotion and progression. *Nat Rev Cancer*. 2023;23(9):600-618.
15. Galeano Nino JL, Wu H, LaCourse KD, et al. Effect of the intratumoral microbiota on spatial and cellular heterogeneity in cancer. *Nature*. 2022;611(7937):810-817. doi:10.1038/s41586-022-05435-0
16. Castellarin M, Warren RL, Freeman JD, et al. *Fusobacterium nucleatum* infection is prevalent in human colorectal carcinoma. *Genome Res*. 2012;22(2):299-306. doi:10.1101/gr.126516.111
17. Kostic AD, Gevers D, Pedamallu CS, et al. Genomic analysis identifies association of *Fusobacterium* with colorectal carcinoma. *Genome Res*. 2012;22(2):292-298. doi:10.1101/gr.126573.111
18. Ou S, Wang H, Tao Y, et al. *Fusobacterium nucleatum* and colorectal cancer: from phenomenon to mechanism. *Front Cell Infect Microbiol*. 2022;12:1020583. doi:10.3389/fcimb.2022.1020583
19. Zepeda-Rivera M, Minot SS, Bouzek H, et al. A distinct *Fusobacterium nucleatum* clade dominates the colorectal cancer niche. *Nature*. 2024;628(8007):424-432. doi:10.1038/s41586-024-07182-w
20. Mima K, Sukawa Y, Nishihara R, et al. *Fusobacterium nucleatum* and T cells in colorectal carcinoma. *JAMA Oncol*. 2015;1(5):653-661. doi:10.1001/jamaoncol.2015.1377
21. Mima K, Nishihara R, Qian ZR, et al. *Fusobacterium nucleatum* in colorectal carcinoma tissue and patient prognosis. *Gut*. 2016;65(12):1973-1980. doi:10.1136/gutjnl-2015-310101
22. Kim HS, Kim CG, Kim WK, et al. *Fusobacterium nucleatum* induces a tumor microenvironment with diminished adaptive immunity against colorectal cancers. *Front Cell Infect Microbiol*. 2023;13:1101291. doi:10.3389/fcimb.2023.1101291
23. Yin H, Miao Z, Wang L, et al. *Fusobacterium nucleatum* promotes liver metastasis in colorectal cancer by regulating the hepatic immune niche and altering gut microbiota. *Aging (Albany NY)*. 2022;14(4):1941-1958. doi:10.18632/aging.203914
24. Bullman S, Pedamallu CS, Sicinska E, et al. Analysis of *Fusobacterium* persistence and antibiotic response in colorectal cancer. *Science*. 2017;358(6369):1443-1448. doi:10.1126/science.aal5240
25. Sakamoto Y, Mima K, Ishimoto T, et al. Relationship between *Fusobacterium nucleatum* and antitumor immunity in colorectal cancer liver metastasis. *Cancer Sci*. 2021;112(11):4470-4477. doi:10.1111/cas.15126
26. Nagtegaal ID, Odze RD, Klimstra D, et al. The 2019 WHO classification of tumours of the digestive system. *Histopathology*. 2020;76(2):182-188. doi:10.1111/his.13975
27. Shigematsu Y, Inamura K, Yamamoto N, et al. Impact of CDX2 expression status on the survival of patients after curative resection for colorectal cancer liver metastasis. *BMC Cancer*. 2018;18(1):980. doi:10.1186/s12885-018-4902-8
28. Shigematsu Y, Tanaka K, Amori G, et al. Potential involvement of oncostatin M in the immunosuppressive tumor-immune microenvironment in hepatocellular carcinoma with vessels encapsulating tumor clusters. *Hepatol Res*. 2024;54(4):368-381. doi:10.1111/hepr.13988
29. Schindelin J, Arganda-Carreras I, Frise E, et al. Fiji: an open-source platform for biological-image analysis. *Nat Methods*. 2012;9(7):676-682. doi:10.1038/nmeth.2019
30. Salter SJ, Cox MJ, Turek EM, et al. Reagent and laboratory contamination can critically impact sequence-based microbiome analyses. *BMC Biol*. 2014;12:87. doi:10.1186/s12915-014-0087-z
31. Kostic AD, Chun E, Robertson L, et al. *Fusobacterium nucleatum* potentiates intestinal tumorigenesis and modulates the tumor-immune microenvironment. *Cell Host Microbe*. 2013;14(2):207-215. doi:10.1016/j.chom.2013.07.007
32. Salama P, Phillips M, Grieu F, et al. Tumor-infiltrating FOXP3+ T regulatory cells show strong prognostic significance in colorectal cancer. *J Clin Oncol*. 2009;27(2):186-192. doi:10.1200/JCO.2008.18.7229
33. Zheng DW, Dong X, Pan P, et al. Phage-guided modulation of the gut microbiota of mouse models of colorectal cancer augments their responses to chemotherapy. *Nat Biomed Eng*. 2019;3(9):717-728. doi:10.1038/s41551-019-0423-2
34. Inamura K. Gut microbiota contributes towards immunomodulation against cancer: new frontiers in precision cancer therapeutics. *Semin Cancer Biol*. 2021;70:11-23. doi:10.1016/j.semcancer.2020.06.006
35. Cao Y, Xia H, Tan X, et al. Intratumoural microbiota: a new frontier in cancer development and therapy. *Signal Transduct Target Ther*. 2024;9(1):15. doi:10.1038/s41392-023-01693-0

SUPPORTING INFORMATION

Additional supporting information can be found online in the Supporting Information section at the end of this article.

How to cite this article: Shigematsu Y, Saito R, Amori G, et al. *Fusobacterium nucleatum*, immune responses, and metastatic organ diversity in colorectal cancer liver metastasis. *Cancer Sci*. 2024;00:1-8. doi:10.1111/cas.16315